SIE 2015
6th International Symposium on Industrial Engineering
24th-25th September 2015
FACULTY OF MECHANICAL ENGINEERING
STEINBEIS ADVANCED RISK TECHNOLOGIES
INNOVATION CENTER FME

INFLUENCE OF XYLAN ON NANOCELLULOSE (NFC) SUSPENSION RHEOLOGY AND AEROGEL MORPHOLOGY

Katarina Dimic-Misic[1], Patrick Gane[1, 2], Tatiana Budtova[3],Christophe Pradille[4], Herbert Sixta [1],Lovikka Ville[1], Thad Maloney[1]

[1]School of Chemical Technology, Department of Forest Products Technology, Aalto University, 00076 Aalto, Helsinki, Finland
[2]Omya International AG, Baslerstrasse 42, CH-4665 Oftringen, Switzerland
[3]CEMEF, Mines Paris Tech, Centre for Material Forming, 06904 Sophia Antipolis cedex, France
4 Mat Xper, 19 Traverse du Barri, 06560, Sophia Antipolis, France

Abstract.*Alkaline washed nanofibrillated cellulose (NFC) samples, obtained via TEMPO-mediation of hardwood Kraft pulp, with different amount of retained xylan were prepared to study the influence of xylan on the water retaining properties of NFC suspensions and on the morphology of dry porous materials derived therefrom by freeze drying. Comparing suspension rheology and dynamic dewatering properties and the morphological and mechanical properties it could be shown that reducing xylan content on NFC results in a weakening gel structure of nanocellulose suspensions and an increase in the mechanical properties of their derived aerogels. Interstitial retained moisture during drying, therefore, leads to weaker interfacial fibrillar bonds.*
Keywords: *nanocellulose, aerogels, rheology, xylan content, water sorption, fibrillar interactions*

1. INTRODUCTION

The potential of NFC materials has been demonstrated with applications, such as reinforcing composites, transparent gas-barrier films [1, 2], medical diagnostics, electronics, cosmetics, aerogels and flame-resistant materials [1-5]. More recently, NFC utilisation in cellulosic aerogel production has been reported [6-8].

Xylan is a hemicellulose abundantly present in hardwoods, where it attaches to cellulose nanofibrils and is present in the cell wall of wood. It has been shown that xylan plays also an important role in the stability of NFC gels [9]. Xylan is located typically on the fibril surfaces and therefore it stabilises the dispersion of NFC both sterically as well as electrically [10],whereas, chemically carboxylated pure cellulose nanomaterials, such as cellulose nanocrystals (CNC) and NFC, are stabilised only electrically, which leads to the solution property dependency on the stability of the gel [10]. This difference could influence significantly the gel-network properties of NFC, which, in both cases, involves trapped and sorbed water.

Flow and dewatering properties of NFC suspensions are important in respect to processability, as they are strongly shear thinning gel-like materials and their viscosity and viscoelasticity properties are concentration and pre-treatment dependent [11, 12]. The swelling radius of a nanocellulose particle is directly related to the charge density caused by the hydroxyl groups, which are in contact with individual water molecules [17]. NFC gels are non-Newtonian fluids, highly dependent on flow conditions, and the increase of shear rate enhances both the aggregation and fragmentation of such complex colloid systems which result in flow curves that have high shear thinning and thixotropic behaviour [18, 19]. Since NFC gels are stabilised with water binding gelation, tuning the gelation mechanism via altering xylan content will have a strong effect on their rheological and dewatering properties.

Aerogels are typically prepared from solvent swollen gels, i.e. percolative networks within a solvent medium, where it is essential that uncontrolled collapse and shrinkage of

thelater network can be suppressed as the solvent is removed. The most widely used technique for the solvent removal is supercritical CO_2 ($scCO_2$)drying or freeze drying. Both $scCO_2$-drying and freeze drying limit shrinkage during the drying process, and the volume fraction of the solid phase in the dry state is similar to that in the wet state. This leads to the characteristic features of aerogels, such as low apparent density, high specific surface area and porosity, as well as low heat conductivity, which makes aerogels useful as catalystsupports, drug delivery vehicles, the basis for novel electrical and magnetic materials, thermal insulators, or as sorbents for oil spills [9].

To investigate dependence of xylan content and consistency on aerogels compressibility, we prepared NFC hydrogels with highest amount of xylan in four different consistencies (1.5 %, 2.4 % and 7.0%) and correspondingly NFC gels with varying amount of xylan at two different consistencies (1.5 % and 4.0%).

2. METHODOLOGY

Never dried laboratory bleached kraft birch pulp (kappa number 0.96) was used as the raw material for the TEMPO-mediated NFC. TEMPO (Sigma Aldrich (St Louis, USA)) was used as catalyst. 13 % NaOCl solution (Merck (Darmstadt, Germany)) was the primary oxidant during the TEMPO-oxidation. 22 g of ortho-boric acid (VWR (Leuven, Belgium)) and 1.8 g of NaOH pellets (VWR (Leuven, Belgium)) were diluted to 2000 cm^3 of distilled water to prepare a borate buffer (pH8.3) in situ. 1 M NaOH (Merck (Darmstadt, Germany)), 1 M HCl (Merck (Darmstadt, Germany)), Büchi reactor (volume 1.6 dm^3), and Metrohm 718 Stat Titrino titrator with pH adjustment were used during the pulp oxidations. All water used in the work was ion-exchanged.

2.1*Alkali treatment of bleached pulps*

Alkaline treatment was applied to the washed birch pulps at room temperature (RT). First, a 0.8 M NaOH solution together with water was added to the pulp to obtain the desired alkalinity and pulp consistency of 5 %. The pulp suspension was then stirred with a mechanical stirrer throughout the reaction time. After the 15 min reaction time, the pulp was washed immediately with deionised water to pH 10-11 and the pH of the suspension was measured with a pH meter (Mettler Toledo). Finally, the pulp was manually pressed to a dry matter content of approximately 20%.

2.2*Preparation and analyses of NFC-TEMPO suspensions*

Radical TEMPO was mixed with NaOCl at a stoichiometrically excess amount in a water solution. The pH level of the solution was adjusted to 7.5 with sulphuric acid. The solution vessel was closed and the solution was mixed until the radical TEMPO was dissolved and converted to its oxidised form due to the formation of HOCl from added NaOCl. The prepared solution was used as a catalyst in the TEMPO-mediated birch pulp oxidation.

The xylan content of the starting birch pulp was reduced with an alkali treatment prior to the TEMPO-mediated oxidation and resulting pulp characterisation. Although alkali treatment is known to change the end product structural and strength-forming properties, the level of alkali treatment was controlled so as not to convert the cellulose I into a cellulose II form in order to minimise any such effects.Then the pulp suspensions were homogenised ready for analysing the resultant NFC gels.

The pulp and the activated TEMPO solution (0.05 mmol TEMPO g^{-1} pulp) were mixed extensively in a closed vessel. Then water and the pulp were added into a Büchi reactor (continuous mixing, temperature 25 °C, volume of pulp solution 1.2 dm^3). 2.4 mmol of NaOCl g^{-1} pulp was added to the Büchi reactor by a pump to adjust the pH level to 9. After the initial addition of NaOCl, the pH of the suspension was kept at 9 with 1 M NaOH additions with an automatic titrator. The oxidation rate was followed by an active chlorine titration until all HOCl from the suspension was consumed.

For rheological measurements 1.5% suspensionsof each sample NFC were used. For aerogel preparation,hydrogels were made at 1.5%, 2%,4 % and 7% consistency for NFC samples without alkaline pretreatment (1,2), and 1.5% and 4% consistency for NFC with alkaline pre-treatment, in order to evaluate the effect of consistency on density and mechanical properties of the resulting aerogels.

2.3*Conversion of residual aldehydes to carboxylates by chlorous acid*

The oxidised pulp suspension at 1 % consistency was adjusted to pH 3 with 1 M HCl. $NaClO_2$ was added to the suspension (1 mM final concentration),forming the acid salt of chlorous acid, and the suspension was mixed in the Büchi reactor for 2 hours at 50 °C. Finally, the pulp was extensively washed with deionised water.

2.4*Surface charge andagglomerate size*

To help characterise the different NFC samples, the charge of the fibrillated cellulose preparedvia different routes (zeta potential (ζ)) was determined by a Zeta-sizer (Malvern Instruments Ltd.). The particle size of the flocculated NFC agglomerates was measured with dynamic light scattering (DLS), using thephoton correlation spectroscopic technique on the same instrument. Prior to measuring the ensemble defined particle size, the samples were diluted with de-ionised water to a solid content of 0.01 %. The scattering volume equivalent diameter (d_{sv}) and ζ are reported as an average of at least five runs. In the case where the density of a material is constant throughout its size distribution, the volume and weight determined size distribution are identical.

2.5 *Fluidisation of TEMPO-oxidised pulp*

The studied TEMPO-oxidised pulp was diluted with water (1.5 % solids) prior to adjusting to pH 9. Then the slurry was homogenised once in a Microfluidics M110P fluidizer through a chamber nozzle pair with diameters of 200 µm and 100 µm at a constant pressure of 1000 bar.

2.6 *Rheology and dynamic dewatering/immobilisation*

The viscoelastic rheological investigations were performed at 23 °C with an Anton Paar 300 (Anton Paar Germany GmbH, Hellmuth-Hirth-Strasse 6, 73760 Ostfildern-Scharnhausen, Germany) oscillatory constant stress/strain and variable shear rheometer [21]. Different types of rheological measurements were performed including viscoelastic measurements, stability and recovery tests (3ITT) and steady state flow with increasing shear rate [12], as well as recording the dynamical change in rheological parameters under dewatering using the immobilisation cell (IMC). To prevent evaporation of the water medium during rheological measurements, a layer of silicone oil was spread over the surface of the sample in contact with the air. All rheological measurements were repeated five times including a pre-shear protocol, and for the calculation of rheological parameters, average values of five measurements are used and quoted with their standard deviation [15, 16].

For the oscillatory measurements a parallel plate geometry with a serrated bottom and upper plate (PP25) was chosen, with diameter of 25 mm, and the gap between upper and bottom plate being set at 1 mm [15, 16]. The pre-shear protocol was applied with an angular frequency of ω = 10 (rad)s^{-1} and strain amplitude γ = 0.01 % for 3 min, followed by a rest time of 10 min [16]. The linear viscoelastic range of the sample (LVE) was obtained from an amplitude sweep oscillatory test using constant angular frequency (ω = 1 (rad)s^{-1}) with varying strain amplitude (γ = 0.01 - 500 %). Dynamic moduli, G' and G'', and complex viscosity (η^*) of the NFC gels were measured as a function of angular frequency (ω) using a downward scaling frequency range (ω = 100- 0.01 (rad)s^{-1}) in frequency sweep oscillatory tests, with a logarithmic spread of data point intervals.Flow curves of NFC gels were measured in a downward shear rate $\dot{\gamma}$ = 1000 – 0.01 s^{-1} with a logarithmic spread of data point duration ranging from 1 to 100 s [12].

Dynamic dewatering measurement was conducted using the same Physica MCR 300 rheometer with IMC accessory as licensed from BASF-AG [15, 16, 64, 71, 72]. A Whatman nucleopore membrane, with the pore size of 0.2 µm, placed on the filter. The upper plate is then lowered into contact with sample [63].NFC suspensions were pre-sheared within the LVE for 20 s, and then the dewatering in DSO proceeded. Determination of immobilisation time, $t_{imm,}$ was calculated as the second zero of damping factor (tan δ)[15].

2.7 *Apparent swelling by WRV measurements*

The swelling of the NFC was determined with a modified version of the solute exclusion test [20]. Two different probe molecules were used in the measurement in order to measure swelling at the interparticle and intraparticle levels. To determine the non-swollen state, 2 x 10^6 Dalton dextran (T2000 from Pharmacosmos) was used for blocking interparticle level swelling. A 5 000 Dalton dextran (T5 from Pharmacosmos) with a Stokes diameter of 3.2 nm was used to block selectively the intraparticle swelling of the NFC. Comparison of the blocked samples with the water-sorbed samples provided a measure of the apparent swelling properties in water.

The network swelling of the nanocellulose was evaluated with a modified water retention value test (WRV ISO/DIS 23714), in order to suit the measurements of gel-like NFC. Due to the difficulty in observing NFC alone as the whole structure change is extremely strong, a dilution with untreated pulp was used as a mix component. The fibre matrix helps in dispersing and filtering the NFC during centrifugation. In the measurement, 5 % NFC was added to a sample of the Birch Kraft bale pulp. The entire sample was measured and the proportional contribution of the NFC was calculated. Samples were measured in duplicate, with agreement between replicate measurements better than ±0.1 cm^3 g^{-1}. Swelling measurements were made under conditions of low conductivity, 15-45 µScm^{-1}, pH 7.5-8.0 and carboxyl groups neutralised in the Na^+ form. Using this methodology, the measurement will more closely reflect the water trapped within the fine scale morphological features of the NFC. A detailed description of the method is provided elsewhere [15, 16].

2.8 *Preparation of Aerogel Membranes*

In order to make NFCfibrils well dispersed, the hydrogel was magnetically stirred for 1 day before use. The specially prepared hollow plastic cylindrical shaped moulds with dimensions about 1.8 – 2.0 cm height and 2 cm diameter, were designed to make NFC gels self-standing structures, Fig.1. Samples were placed in a Cryothec Freeze dryer with the temperature of the cool trap being -80 °C and an end pressure of -40 mTorr.Due to the vacuum pumping action, the sample quickly cools below the freezing point of water by the induced evaporation of liquid water in the form of vapour, and thereafter the water is removed from the frozen state by sublimation[11]. After complete water removalwhitesponge-like aerogels with a very low density are obtained.

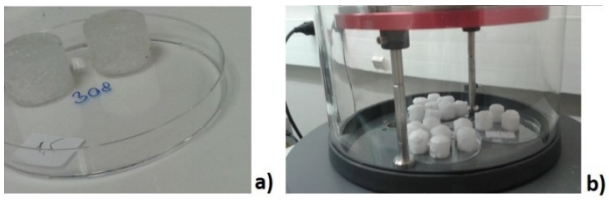

Fig.1 Preparation of NFC aerogels from hydrogels: a)plastic cylindrical moulds withholes were made to hold low and high consistency hydrogels, and b) enabling formation of self-standing structures of aerogels for freeze drying.

2.9*Scanning electron microscopy*

Scanning electron microscopy (SEM) imaging was performed using A PHILIPS XL 30 on samples covered with gold, under vacuum at the acceleration voltage of 15 kV for 1 min.The specimens were made directly from breaking the cylinder mould into two parts and using fresh fracture surfaces in order to investigate the aerogel inner surface.

Densities of the aerogels were calculated by weighing the samples and measuring the volumes.

2.10*Nitrogen-adsorption-desorption measurements*

The specific surface areas were determinated by nitrogen adsorption carried out in a Coulter Omnisorp 100CX at the temperature of liquid nitrogen. Before measurements the samples were dried at the temperature of 100 °C until the vacuum of 1×10^{-5} Torr was reached. Both adsorption and desorption isotherms were measured and the surface area was determined from the adsorption curve by the Brunauer–Emmet–Teller (BET) method. The mesopore diameter distributions were determined from desorption isotherms by the Barret–Joyner–Halenda (BJH) method assuming open cylindrical pores[29]. The limit of accuracy is 1%.

2.11*Mechanical testing*

Uniaxial compression tests were carried out on a tensile testing machine Zwick (Zwick GmbH, Germany) Z 2.5 equipped with a 2.0 load cell according to ISO 604 with the testing speed of 1mmmin^{-1} and a preload of 1N. Teflon plates were mounted on the compression tools in order to minimise the friction. Strains were calculated as a ratio of displacement of the machine plates over nominal height of a sample. All samples were conditioned for at least 72 h prior to testing in a controlled environment (23 °C, 50% RH) according to ISO291. At least 5 samples of each formulation were tested. The error in compression modulus was 20%. Relative compression modulus E_{rel} was calculated as a ratio of the absolute compression modulus and density of the sample in gm^{-3} allowing suppression of the influence of sample density on the mechanical properties of a composite. The Poissonratio was calculated as a negative ratio of transverse to axial strain. The strains were measured from images taken using a fixed optical camera during testing.

3. RESULTS AND DISCUSSION

3.1*Removal of Xylan and TEMPO-mediated Oxidation*

Alkalitreatment of bleached birch pulp was conducted at room temperature at 5 % pulp consistency for 15 min which is sufficient reaction time due to the fast xylan removal which was earlier reported to take place immediately (e.g. 1 min) after NaOH is exposed to the pulp [29]. The xylan content decreased linearly as a function of NaOH concentration from 25.2 % to 7.3 % (NaOH concentration varied between 0 – 2 M, as presented in Table1. The removal of xylan correlates with increasing alkali concentration of alkali treatment with birch pulp correspondingly to earlier study [26, 27,29]

Table 1TEMPO-mediated pulp oxidations of alkalitreated (AT) and reference bleached birch pulps and description of NFC with different alkali treatment.

Sample name	Ref.	AT/0.75	AT/1	AT/1.5	AT/2	BC
Alkali treatment / mmol dm^{-3} NaOH	0	0.75	1.0	1.5	2.0	N.A.
Xylan content after alkali treatment / %	25.2	19.9	15.3	10.6	7.3	N.A.
Reaction time of TEMPO oxidation /min	220	132	80	51	28	N.A.
Carboxylate content /mmol g^{-1} pulp	0.89	0.90	0.93	0.85	0.90	0
Carboxylate + aldehyde content /mmol g^{-1} pulp	0.97	1.03	1.06	1.11	1.17	N.A.

Reaction time of TEMPO-mediated oxidation reduces with the decreasing xylan content of pulp. Increased reactivity of alkali treated cellulose is proposed to be dependent onthe content of dissolved xylan as well as on the alkali-induced swelling of the fibre wall [29]. Reaction times are higher compared with earlier reported results under similar conditions [29]. However, in this case the reference pulp contains higher xylan content (25.2 %) compared withthe corresponding reference pulp (22.4 %) reported earlier [29].

The fibrillar structure of NFC-gels produced from xylan extracted (alkali washed) TEMPO-oxidised pulps was studied with atomic force microscopy (AFM). The AFM images were recorded from the dried NFC-gel samples without any fractionation having been applied in order to maintain the actual fibrillar structure of the produced NFC gel. The AFM images revealed clearly that all pulps were fibrillated effectively down to the individual fibril scale, when excluding observed large fibril flocs.

The AFM imaging was utilised also for measuring the fibril dimensions in the produced NFC-gels. The AFM technique gives only values relevant to theprobe *z*-direction motion due to the image artefacts related to the AFM technique [2, 11].

Table 2 Measured thicknesses for fibril dimensions with AFM. AW denotes the alkali washed samples with alkali concentration 0.75-2.0 mol NaOH dm^{-3}. BC denotes bacterial cellulose sample.

Sample name	Ref	AW/0.75	AW/1.0	AW/1.5	AW/2.0	BC
Thickness of fibril (nm)	4.0 ± 1.1	3.4 ± 0.8	3.6 ± 0.5	2.9 ± 0.4	3.1 ± 0.6	0.5 ± 0.1

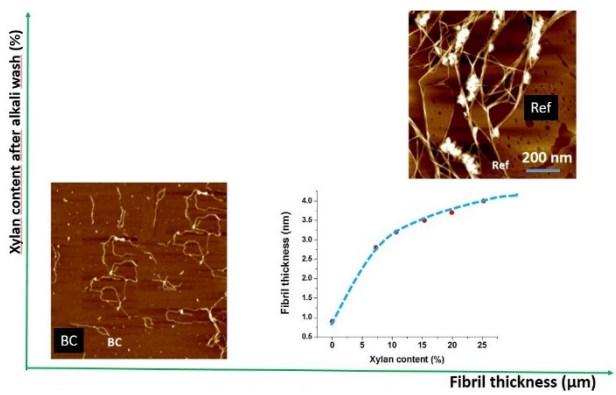

Fig 2. NFC fibril thickness as a function of xylan content

3.2 *Swelling and water retention (WR)of NFC*

A thorough description of the swelling of an NFC gel should include both the water trapped within the interstitial fibrillary matrix and within each fibril. The network swelling of the NFC increases strongly with xylan content. The xylan appears to stabilise the NFC network sterically thus immobilising water in the interstitial spaces. Interestingly, the xylan content, dominates over the increase in charge in the TEMPO oxidised series as the acid content increased from 0.97 to 1.17 $mmolg^{-1}$ through the series, while the network swelling decreased from 14.3 to 6.0 cm^3 g^{-1}. Other factors being equal, increasing surface charge will increase swelling

.

Table 3 Particle and network swelling as a function of xylan and COOH content, showing the strong effect of xylan hemicellulose on trapping the water within the nanofibrillar matrix.

NFC suspension	**Particle swelling** 3.2 nm dextran probe/ cm^3g^{-1}	**Network swelling** 54.0 nm dextran probe/ cm^3g^{-1}	**WRV** / g_{water} g^{-1}_{NFC}	**Filtrate amount during static dewatering** ÅA GWR/ gm^{-2}
Ref	2.7	14.3	10.8	404.2
AW/0.75	2.8	13.7	9.6	620.4
AW/1	2.2	11.4	N.A.	621.2
AW/1.5	1.7	8.6	10.3	724.1
AW/2	1.9	6.0	5.5	1 903.6
BC	0.5	3.2	N.A.	8 643.4

3.3 *Rheology*

Oscillatory measurements presented in Figs.3a) and b) were used to characterise the difference of microstructure of nanocellulose suspensions throughout the LVE domain[1, 12, 14, 15].The first observation we make from Fig.3a) is that there is an obvious difference between samples regarding the xylan content, as two distinct groups of *G′* and *G′′* can be distinguished. The upper one with nanofibrillar celluloses contains high and medium amounts of xylan, respectively, i.e. Ref, AW/0.75, AW/1 and AW/1.5, with γ_c at 0.2 %. The second group shows lower values of "wavy" shaped *G′*and *G′′* for nanofibrillar cellulose suspensions having drastically reduced xylan content, AW/2, and no xylan, BC. The longer LVE[16] for nanofibrillar cellulose suspensions in the firstgroup is explained by the stronger gel-like structure build between the more swollen fibrils with higher carboxylic content on their surface, [12, 16],showing different agglomeration

mechanisms between those two distinguished groups. Similarly, difference in strength of nanocellulose gel is observable from frequency sweep measurements, Fig 3b), expressed as independence of $G'$and G'' from frequency for small frequencies and increase for higher frequencies, respectively again, according to the distinguished grouping of suspensions regarding xylan content. The elastic behaviour of the samples predominates over viscous, with rigidity increase with frequency being more pronounced for nanofibrillar cellulose of the second group (AW2 and BC), also explained as strain hardening, possibly due to increasing friction within less swollen nanocelluloses at higher frequencies [27, 13, 15, 16].

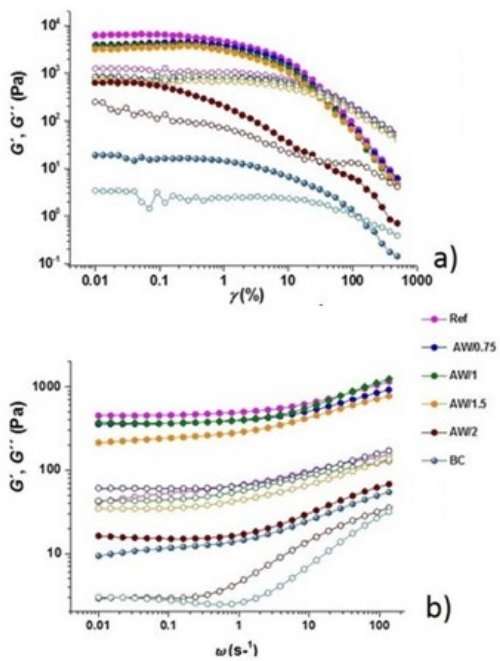

Fig. 3 Viscoelastic measurements for NFC suspensions: a) amplitude sweep for a range of strain (γ = 0.01-500 %) at constant angular frequency of 1 (rad)s^{-1}, b) frequency sweep (0.1-100 (rad)s^{-1}) at constant strain of 0.1 %.Elastic modulus (G') are presented with open symbols, loss modulus (G'') with closed symbols.

The immobilisation curves in Fig.4 display a clear difference in the rate and nature of immobilisation in relation to partial/total removal of xylan in the suspension matrix. The increase of elasticity (G') of the structure, and can be traced through the difference in moduli (G' and G''), which is more pronounced for the samples which have xylan remaining in suspensions, in contrast to those without xylan [21]there follows a decrease, probably due to smaller, less swollen and more mobile, gel-liberated nanocellulose particles. We see that, (i) with reducing amount of xylan there is an obvious difference in dynamic of development of viscoelastic moduli (G' and G'') and the suspensions with larger xylan content immobilise as gel ($G'>G''$), which is opposite for the other, low-xylan content group. After initial dewatering, bound water in the second group, leaves the suspension, which results in elasticity decrease after immobilisation.

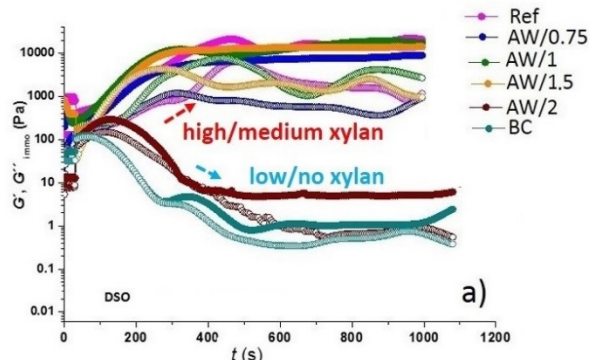

Fig. 4 Determination of nanocellulose suspension dewatering using dynamic dewatering (IMC) in DSO mode as a function of dewatering time, showing the change of the amount of entrapped gel water within the filter cake upon immobilisation.

As the presence of xylan affects the nature of immobilisationwe highlight the grouping of nanofibrillar cellulose suspensions giving correlation between swelling as seen in Fig. 3 and its influence on dewatering as seen in Fig. 4, indicating that by reducing xylan structure there is a lower level of gel-water trapping, which naturally reduces elasticity within the suspension.

3.4*Aerogels*

Instead of traditionally used supercritical CO_2 drying, which includes solvent exchange, here we used afreeze drying method to remove water directly from the aqueous gel, as described earlier by Pääkko [11] where moulds with hydrogels samples were placed in a vacuum oven without any preceding freezing.Due to the vacuum pumping action, the samples quickly cool below thefreezing point of water, and afterwards water is removed by sublimation. It has been demonstrated that such gels have very low porosity and a layered sheet structure with micropores and mesopores. Using this method part of the water is evaporated already from the liquid state during the initial state of pumping.Theremaining part of the water is sublimated from the frozen state. Fig. 5 presents the SEM images from the sponge-like aerogels, which have very high porosity ~ 98%[11, 12].The specific BET surface area was in range 9-11 m^2g^{-1}. When aerogel structure is formed from the sheet-like skeleton, the sheets are inter-connected by fibrillar joint networks and are able to deform readily [12].

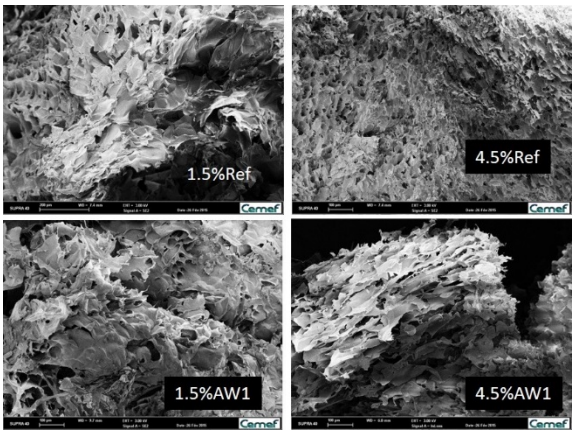

Fig5. SEM images from aerogels as a function of solids content.

Representative compression stress-strain curves for Ref samples, for all four different consistencies, are presented in Fig. 6a). For higher consistencies, 4 % and 7%, it is evident that a linear increase in stress as a function of strainis followed by a plastic deformation region and then a sharp increase upon densification of the porous structure. The stress-strain curve shows that the stiffness of aerogels increases with increase in consistency. The dependence of compressive modulus as a function of density, presented in Fig. 6b), reveals that, as seen in Fig. 6a), density (solids content) has a strong influence on the compressive moduli of the aerogels, while elasticity is higher as the xylan content decreases, as seen for all samples at both 1.5 % and 4 %.

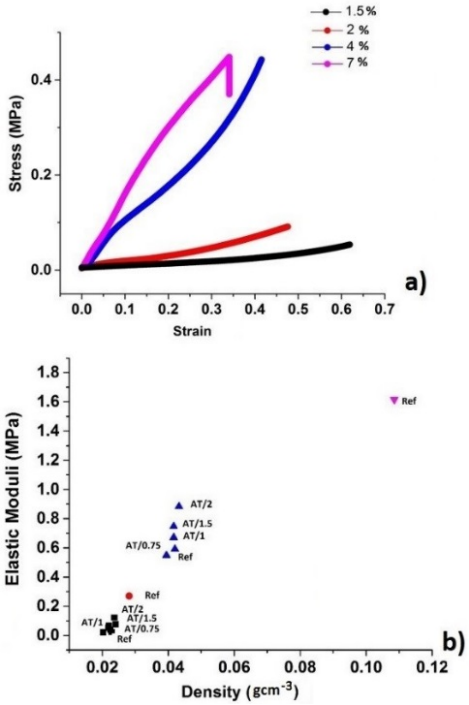

Fig. 6 Compression stress-strain curve for freeze-dried aerogels: a) made from Ref samples, and b) dependence of elastic (compression) moduli on density for all samples.

The lower amount of xylan in the aerogel network results in higher compressive modulus due to the evident influence on the nanocellulose network, which has swollen xylan bundles between nano-fibrils. Image analysis of compressed aerogels, Fig. 7, viewed from the beginning of compression through the end compression (last of four images) of 7 %.

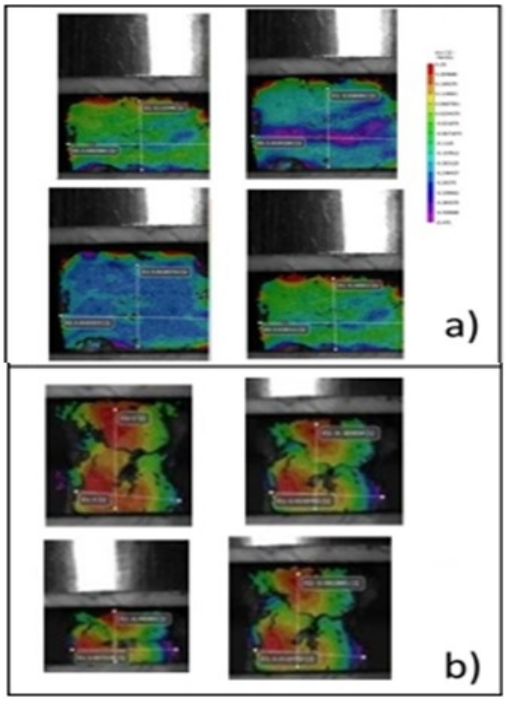

Fig 7. Stress distribution images of compressibility of Ref samples at a) 7.0%, and b) 1.5% consistency.

4. CONCLUSIONS

In the present work, the role of xylan on the water binding properties of NFC gels is investigated through the rheological and dynamic dewatering behaviour of nanocellulose gels with varying xylan content. The xylan is water binding polysaccharide and is attached to fibrils, surviving the TEMPO-oxidation, unless it is removed by alkaline pre-treatment. The effect of xylan on the amount of immobilised water within NFC gels is correlated through the different strengths of the gels, as the mechanical structure of water-interlocking aggregates of xylan is preventing structure collapse upon dynamic dewatering. The role of xylan removal on the strength of NFC aerogels is seen through the increase of compression moduli with decrease of xylan content, which is in turn is consistency dependent.

Acknowledgements: The authors are grateful to Dr. Nela Buchtova for her assistance in the preparation of aerogels and assistance with the work performed at CEMEF, France.

REFERENCES

[1] Agoda-Tandjawa G, Durand S, Berot S, Blassel C, Gaillard C, Garnier C. Rheological characterization of microfibrillated cellulose suspensions after freezing. Carbohydr Polym. 2010 5/5;80(3):677-86.

[2] Anelli PL, Biffi C, Montanari F, Quici S. Fast and selective oxidation of primary alcohols to aldehydes or to carboxylic acids and of secondary alcohols to ketones mediated by oxoammonium salts under two-phase conditions. J Org Chem. 1987 06/01; 2013;52(12):2559-62.

[3] Araki J, Wada M, Kuga S. Steric stabilization of a cellulose microcrystal suspension by poly (ethylene glycol) grafting. Langmuir. 2000, 17(1):21-7.

[4] Bulota M, Vesterinen A, Hughes M, Seppälä J. Mechanical behavior, structure, and reinforcement processes of TEMPO-oxidized cellulose reinforced poly(lactic) acid. Polymer Composites. 2013;34(2):173-179.

[5] Chen W, Li Q, Wang Y, Yi X, Zeng J, Yu H Comparative study of aerogels obtained from differently prepared nanocellulose fibers. Chem Sus Chem. 2014;7(1):154-61.

[6] Jin, H., Kettunen, M., Laiho, A., Pynnönen, H., Paltakari, J., Marmur, A.,Illala O, Ras, R. H. Superhydrophobic and superoleophobic nanocellulose aerogel membranes as bioinspired cargo carriers on water and oil. Langmuir, 2011,27(5), 1930-1934.

[7] de Nooy AEJ, Besemer AC, van Bekkum H. Selective oxidation of primary alcohols mediated by nitroxyl radical in aqueous solution. Tetrahedron. 1995 7/17/;51(29):8023-32.

[8] Dimic-Misic K, Nieminen K, Gane P, Maloney T, Sixta H, Paltakari J. Deriving a process viscosity for complex particulate nanofibrillar cellulose gel-containing suspensions. Appl. Rheol. 2014; 24:35616-25.

[9] Kitaoka T, Isogai A, Onabe F. Chemical modification of pulp fibers by TEMPO-mediated oxidation. Nord Pulp Pap Res J. 1999;14(4):279-84.

[10] Koga H, Saito T, Kitaoka T, Nogi M, Suganuma K, Isogai A. Transparent, conductive, and printable composites consisting of TEMPO-oxidized nanocellulose and carbon nanotube. Biomacromolecules. 2013 02/22; 2014; 14(4):1160-5.

[11] Läuger J, Wollny K, Huck S. Direct strain oscillation: a new oscillatory method enabling measurements at very small shear stresses and strains. Rheol Acta. 2002;41(4):356-61.

[12] Lee K, Bismarck A. Susceptibility of never-dried and freeze-dried bacterial cellulose towards esterification with organic acid. Cellulose. 2012, 19(3):891-900.

[13] Lowys M, Desbrieres J, Rinaudo M. Rheological characterization of cellulosic microfibril suspensions. role of polymeric additives. Food Hydrocoll. 2001;15(1):25-32.

[14] Meng Q, Li H, Fu S, Lucia LA. The non-trivial role of native xylans on the preparation of TEMPO-oxidized cellulose nanofibrils. React Funct Polym. 2014;85 :142-50.

[15] Naderi A, Lindström T, Pettersson T. The state of carboxymethylated nanofibrils after homogenization-aided dilution from concentrated suspensions: A rheological perspective. Cellulose. 2014;21(4):2357-68.

[16] O`Brien F J, Harley B A, Yannas IY, Gibson L. Influence of freezing rate on pore structure in freeze-dried collagen-GAG scaffolds. Bioaterials, 2004 (25);1077-1086.

[17] Okita Y, Saito T, Isogai A. TEMPO-mediated oxidation of softwood thermomechanical pulp. Holzforschung. 2009 2013-09-13;63:529-35.

[18] Duchesne I, Hult E, Molin U, Daniel G, Iversen T, Lennholm H. The influence of hemicellulose on fibril aggregation of kraft pulp fibres as revealed by FE-SEM and CP/MAS 13C-NMR. . 2001;8(2):103-111.

[19] Puisto A, Illa X, Mohtaschemi M, Alava M. Modeling the viscosity and aggregation of suspensions of highly anisotropic nanoparticles. Eur Phys J E. 2012;35(1):1-7.

[20] Tenhunen T, Peresin MS, Penttilä PA, Pere J, Serimaa R, Tammelin T. Significance of xylan on the stability and water interactions of cellulosic nanofibrils. React Funct Polym. 2014;85(0):157-66.

[21] Wollny K. New rheological test method to determine the dewatering kinetics of suspensions. Appl Rheol. 2001;11(197):202.